

# Excited-State Energy Dynamics of Conjugated Polycarbogermane Oligomers: Introduction Effects of Germanium Atom into $\pi$ -Conjugated Molecular System

SANG HO CHOI,<sup>1</sup> IN-WOOK HWANG,<sup>1</sup> SUNG HEE KIM,<sup>1</sup> YOUNG TAE PARK,<sup>2</sup> YONG-ROK KIM<sup>1</sup>

<sup>1</sup> Department of Chemistry, Yonsei University, Shinchon-Dong 134, Seodaemun-Gu, Seoul 120-749, Korea

<sup>2</sup> Department of Chemistry, Keimyung University, Taegu 704-701, Korea

Received 21 March 2001; revised 4 April 2002; accepted 4 April 2002

**ABSTRACT:** Excited-state energy dynamics of the conjugated polycarbogermane oligomers, poly{[1,4-bis(thiophenyl)buta-1,3-diyne]-*alt*-(dimethylgermane)} (PBTBD-DMG;  $n = 33$ ), poly{[1,4-bis(thiophenyl)buta-1,3-diyne]-*alt*-(diphethylgermane)} (PBTBD-DPG;  $n = 12$ ), poly{[1,4-bis(phenyl)buta-1,3-diyne]-*alt*-(dimethylgermane)} (PBPBD-DMG;  $n = 36$ ), and poly{[1,4-bis(phenyl)buta-1,3-diyne]-*alt*-(diphenylgermane)} (PBPBD-DPG;  $n = 2$ ), were investigated by steady-state and picosecond time-resolved fluorescence spectroscopies in liquid solution. The introduction effect of a germanium atom into  $\pi$ -conjugated oligomer backbones and the substitution effect of a methyl or phenyl group on the germanium atom are discussed from solvent polarity-dependent studies. Steady-state and time-resolved fluorescence studies on the thiophene-containing polycarbogermane (PBTBD-DMG and PBTBD-DPG) oligomers revealed considerable solvent polarity-dependent characteristics, whereas those of the phenylene-containing polycarbogermane (PBPBD-DMG and PBPBD-DPG) oligomers do not significantly show such characteristics. As the solvent polarity increased from *n*-hexane to tetrahydrofuran, the steady-state fluorescence spectra of PBTBD-DMG and PBTBD-DPG oligomers were significantly redshifted, and their fluorescence lifetimes seemed to change from  $\sim 624$  to  $\sim 46$  ps. These results suggest that the excited-state dynamics of PBTBD-DMG and PBTBD-DPG oligomers are related to an intramolecular charge transfer (ICT) emission process through (d-p)  $\pi$  conjugation between the  $\pi$ -conjugated system and unoccupied 4d orbitals of the germanium atom. These results are supported by quantum chemical (AM1 and CNDO/2) calculations. © 2002 Wiley Periodicals, Inc. *J Polym Sci Part B: Polym Phys* 40: 1298–1306, 2002

**Keywords:** photophysics; fluorescence; charge transfer; (d-p)  $\pi$  conjugation

## INTRODUCTION

The optical properties of photoexcited polyacetylene,<sup>1</sup> polythiophene,<sup>2</sup> and polyphenylene have provided important information on their possible

applications of a nonlinear optical device<sup>3</sup> and their roles as model compounds for quasi-one-dimensional semiconductors.<sup>4</sup> Also, the importance is that the densities of such polymers (generally ca. 1 g/cm<sup>3</sup>) are much lower than those of the metals (8.92 g/cm<sup>3</sup> for copper and 19.3 g/cm<sup>3</sup> for gold), which makes them attractive for the applications where weight is an important factor.<sup>5</sup> Typical applications include light-weight batteries,<sup>6</sup> thin-film transistors,<sup>7</sup> light-emitting diodes,<sup>8</sup> and photovoltaic cells.<sup>9</sup> Such properties

Correspondence to: Y.-R. Kim (E-mail: yrkim@alchemy.yonsei.ac.kr)

*Journal of Polymer Science: Part B: Polymer Physics*, Vol. 40, 1298–1306 (2002)  
© 2002 Wiley Periodicals, Inc.

can also be tuned by changing the molecular compositions of the polymers.

Various studies have been performed on the modifications of the chain units or the substituents and the preparations of copolymers to obtain the molecular properties for their specific applications and to examine the rules governing energy-transport properties in these polymeric materials.<sup>10</sup> Among them,  $\pi$ -conjugated copolymers including silicon subgroup elements (Si, Ge, and Sn) have recently raised both scientific and technological interests because of their optoelectronic properties applicable to photoresists,<sup>11</sup> conductive materials,<sup>12</sup> and electroluminescent layers in large-area light-emitting diodes.<sup>13</sup> The electrical conductivity and high thermal property were observed in conjugated polycarbosilanes and polycarbogermans, such as poly(silylenediacylenes) and poly(germylenediacylenes).<sup>14,15</sup> In these polymers, the copolymer backbones exhibit  $\pi$  conjugation, whereas silicon subgroup elements were considered to decouple the intrinsic  $\pi$  conjugation between two adjacent copolymer backbone units. However, according to previous studies of polycarbosilanes,  $\pi$  conjugation can be extended through the silicon atom via (d-p)  $\pi$  conjugation<sup>16–18</sup> and/or  $\sigma, \pi$  hyperconjugation<sup>20</sup> in  $\pi$ -conjugated copolymers including silicon atoms. However, there are no detailed studies on  $\pi$ -conjugated copolymers including the germanium atom, which is in the same subgroup as silicon, although knowledge of their photophysical properties can be interesting because of the similar electronic configuration but larger atomic size than that of the silicon atom.

In this study, the introduction effect of the germanium atom into  $\pi$ -conjugated oligomer backbones and the dimethyl or diphenyl substitution effect on the germanium atom are discussed from the viewpoint of charge-transporting dynamics, and the solvent-polarity effects on the fluorescence spectra of these polycarbogermane oligomers are investigated in both polar [tetrahydrofuran (THF)] and nonpolar (*n*-hexane) solvents at room temperature. Quantum chemical calculations (AM1<sup>21</sup> and CNDO/2<sup>22</sup>) were performed to support the experimental results.

## EXPERIMENTAL

Soluble polycarbogermane oligomers without long alkyl or alkoxy chains were chemically synthesized to investigate their charge-transporting dy-

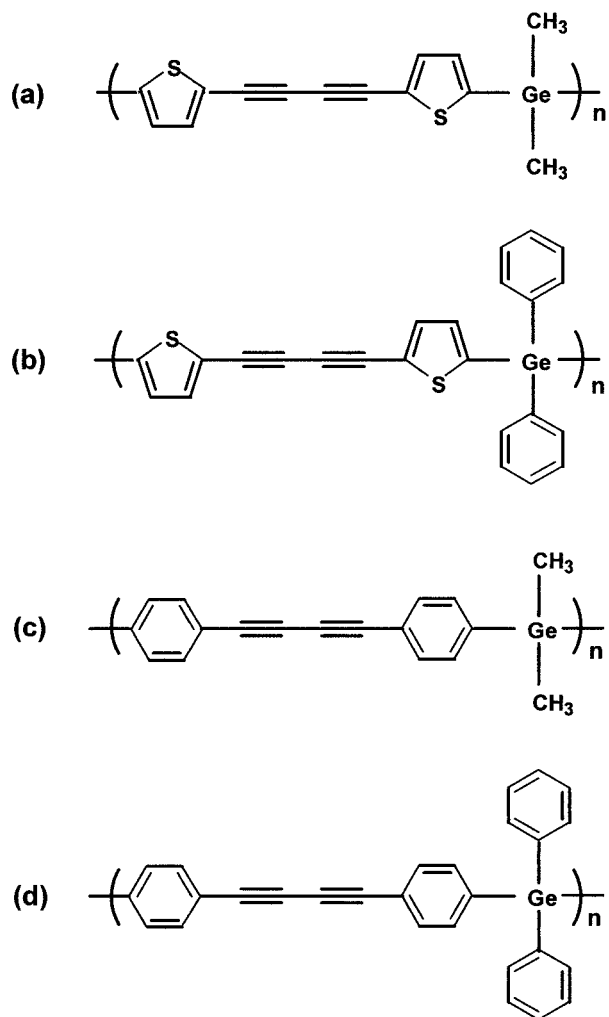


**Figure 1.** Chemical structures of (a) PBTBD-DMG ( $n = 33$ ), (b) PBTBD-DPG ( $n = 12$ ), (c) PBPBD-DMG ( $n = 36$ ), and (d) PBPBD-DPG ( $n = 2$ ), where  $n$  represents the repeating unit numbers in the oligomers.

namics. Full details of the syntheses and characterizations of the monomers and oligomers have been reported in the literature.<sup>15</sup> The chemical structures of the oligomers are given in Figure 1.

The degree of polymerization,  $n$ , of poly{[1,4-bis-(thiophenyl)buta-1,3-diyne]-*alt*-(dimethylgermane)} (PBTBD-DMG;  $n = 33$ ), poly{[1,4-bis-(thiophenyl)buta-1,3-diyne]-*alt*-(diphenylgermane)} (PBTBD-DPG;  $n = 12$ ), poly{[1,4-bis(phenyl)buta-1,3-diyne]-*alt*-(dimethylgermane)} (PBPBD-DMG;  $n = 36$ ), and poly{[1,4-bis(phenyl)buta-1,3-diyne]-*alt*-(diphenylgermane)} (PBPBD-DPG;  $n = 2$ ) oligomers is about 33, 12, 36 and 2, respectively. These values were estimated by the molecular weight averaging method from the results of gel permeation chro-

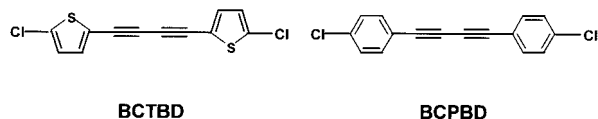


**Figure 2.** Chemical structures of BCTBD and BCPBD.

matography. 1,4-Bis(5-chlorothiophenyl)buta-1,3-diyne (BCTBD) and 1,4-bis(5-chlorophenyl)buta-1,3-diyne (BCPBD) monomers were also prepared for comparative studies, and the model compounds of the chemical structures are displayed in Figure 2. BCTBD and BCPBD monomers are quite similar to the repeating unit of the main chain of PBTBD and PBPBD oligomers in their chemical structures, respectively.

The solution samples were prepared in *n*-hexane [high-pressure liquid chromatographic (HPLC) grade; Merck] and THF (HPLC grade; Merck) for steady-state and time-resolved fluorescence spectroscopic studies. Their concentrations were maintained at less than  $10^{-4}$  M where there was no concentration dependence on the spectrum, and all experiments were performed at room temperature. Steady-state fluorescence spectra were obtained by a spectrofluorimeter (Hitachi F-4500), and a picosecond time-correlated single photon-counting (TCSPC) system was used for the measurement of time-resolved fluorescence-decay profiles. The TCSPC laser system used in this study consists of a cavity-dumped dye laser that is synchronously pumped by a mode-locked Nd-YAG laser (Antares 76-YAG, Coherent). More detailed information on the TCSPC system has been given in a previous report.<sup>23</sup> The temporal pulse width of the excitation radiation was 2–3 ps, and the excitation wavelength was 298 nm. The full width at half-maximum of the instrument response function (IRF) was 74 ps. The exponential fittings were done with an iterative least-squares deconvolution fitting procedure. The fluorescence decays were measured at several fixed emission wavelengths over spectral regions with the magic-angle polarization of emission.

Semiempirical calculations were performed on an IBM586-type computer using MOPAC97.<sup>24</sup> The quantum chemical calculations for the repeating units of PBTBD-DMG and PBPBD-DMG oligomers were performed at the AM1 and CNDO/2 level.

## RESULTS AND DISCUSSION

### Absorption and Fluorescence Properties

PBTBD-DMG, PBTBD-DPG oligomers [Figs. 1(a,b)], and BCTBD monomer (Fig. 2) include the thiophene group in the  $\pi$ -conjugated backbone, whereas PBPBD-DMG, PBPBD-DPG oligomers [Figs. 1(c,d)], and BCPBD monomer (Fig. 2) contain the phenylene group in the  $\pi$ -conjugated backbone. The steady-state fluorescence spectra of the conjugated polycarbogermanes and their monomer-sized compounds in *n*-hexane and THF solvents are depicted in Figure 3, along with the absorption spectra. In the cases of PBTBD-DMG and PBTBD-DPG oligomers, the fluorescence spectra of the oligomers in Figures 3(b,c) are significantly redshifted and structureless as compared with the spectra of BCTBD monomer [Fig. 3(a)] in nonpolar (*n*-hexane) solvents. Also, the absorption bands at the longer wavelength regions, which do not appear in the absorption spectra of BCTBD monomer, are newly appeared in the polymeric states. The conjugation effect through the oligomer backbones apparently exists. On the other hand, as shown in Figures 3(e,f), the spectra of PBPBD-DMG and PBPBD-

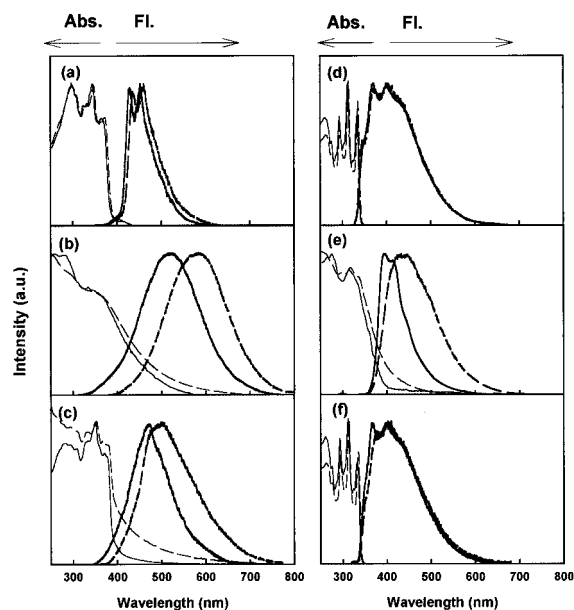


**Figure 3.** Steady-state absorption and fluorescence spectra (bold line) of (a) BCTBD ( $n = 1$ ), (b) PBTBD-DMG ( $n = 33$ ), (c) PBTBD-DPG ( $n = 12$ ), (d) BCPBD ( $n = 1$ ), (e) PBPBD-DMG ( $n = 36$ ), and (f) PBPBD-DPG ( $n = 2$ ) in *n*-hexane (solid line) and THF (dotted line). The excitations were at 298 nm.

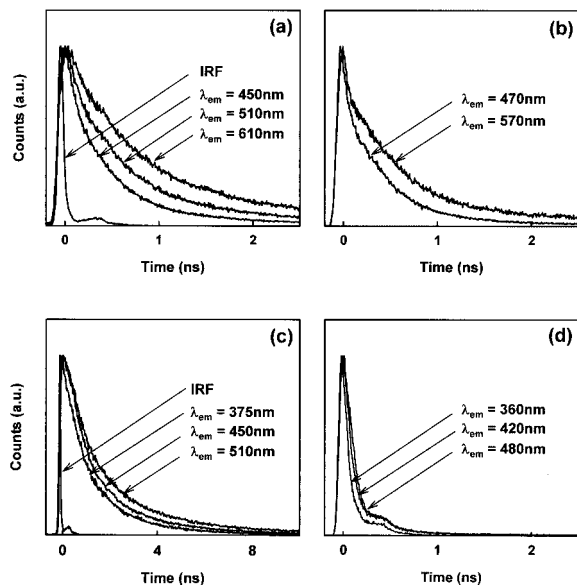


**Figure 4.** Picosecond fluorescence decay profiles of (a) PBTBD-DMG, (b) PBTBD-DPG, (c) PBPBD-DMG, and (d) PBPBD-DPG oligomers in *n*-hexane. IRF represents the instrumental response function of the TC-SPC system.

DPG oligomers are relatively similar to that [Fig. 3(d)] of their monomer-sized compound (BCPBD) in their spectral structures and energies. It suggests that the presence of a germanium atom between the phenylene-diacetylene backbone units results in the more-effective interruption of  $\pi$  conjugation. Of course, it is difficult to compare their spectra to each other because the chain length of PBPBD-DPG oligomer ( $n = 2$ ) is much shorter than those of the others ( $n = 33, 12,$  and  $36$ ). However, because the spectra of PBPBD-DPG oligomer are still very similar to those of BCPBD monomer although the chain length of that oligomer is approximately twice longer than that of BCPBD monomer, indicating that the effective conjugation length of PBPBD-DPG oligomer is smaller than  $n = 2$ , it can be still considered that the more-effective interruption of  $\pi$  conjugation as a result of the germanium atom in the backbone occurs in PBPBD-DPG oligomer.

In Figure 3, as the solvent polarity increases from *n*-hexane to THF, the Stokes shifts in the fluorescence spectra are generally larger in the thiophene-containing monomer and polycarbo-germanane oligomers (BCTBD, PBTBD-DMG, and PBTBD-DPG) than the phenylene-containing compounds (BCPBD, PBPBD-DMG, and PBPBD-DPG). For PBPBD-DPG oligomer, it cannot be

excluded that the low chain length ( $n = 2$ ) of the oligomer may cause the consistency of the steady-state fluorescence spectra in *n*-hexane and THF. However, from the fact that the Stokes shift in the fluorescence spectrum of BCTBD monomer ( $n = 1$ ) is larger than that in the fluorescence spectrum of PCPBD monomer ( $n = 1$ ), such large Stokes shifts indicate that the excited states of the thiophene-containing compounds (BCTBD, PBTBD-DMG, and PBTBD-DPG) are more polar than those of the phenylene-group-containing compounds (BCPBD, PBPBD-DMG, and PBPBD-DPG).

Presumably, it is contributed by the empty 4d orbital of germanium to the  $\pi$  systems of the backbone, which has also been observed in silicon-atom-containing  $\pi$ -conjugated polymers.<sup>25,26</sup> This is discussed in detail in the following fluorescence kinetic studies.

### Excited-State Temporal Decays

Picosecond time-resolved fluorescence-decay profiles of PBTBD-DMG, PBTBD-DPG, PBPBD-DMG, and PBPBD-DPG oligomers in each solvent are portrayed in Figure 4 (*n*-hexane) and Figure 5 (THF). In Figures 4 and 5, the decays of PBTBD-DMG and PBTBD-DPG oligomers become faster with increasing solvent polarity, whereas those of PBPBD-DMG and PBPBD-DPG oligomers that

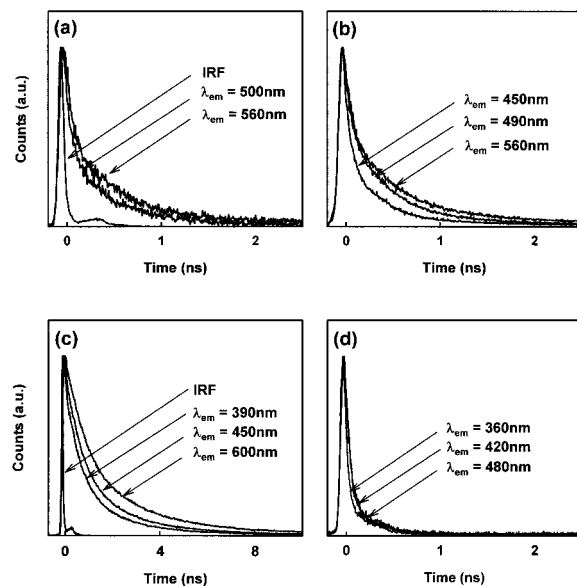


**Figure 5.** Picosecond fluorescence-decay profiles of (a) PBTBD-DMG, (b) PBTBD-DPG, (c) PBPBD-DMG, and (d) PBPBD-DPG oligomers in THF solution.

**Table 1.** Fluorescence Lifetimes of Conjugated Polycarbogermane Oligomers

Sample	Solvent	$\lambda_{em}$ (nm)	$\tau_1$ (ps)	$\tau_2$ (ps)	$\tau_3$ (ps)	$\chi^2$
PBTBD-DMG	<i>n</i> -Hexane	450	200 (74%)	630 (18%)	2000 (8%)	1.2
	<i>n</i> -Hexane	500	205 (53%)	622 (38%)	1962 (9%)	1.1
	<i>n</i> -Hexane	610	197 (40%)	642 (40%)	1741 (20%)	1.0
PBTBD-DPG	<i>n</i> -Hexane	470	200 (73%)	605 (22%)	2700 (5%)	1.2
	<i>n</i> -Hexane	570	195 (52%)	620 (38%)	2850 (10%)	1.1
PBPBD-DMG	<i>n</i> -Hexane	375	132 (32%)	874 (48%)	2752 (10%)	1.2
	<i>n</i> -Hexane	450	148 (15%)	849 (63%)	2825 (23%)	1.2
	<i>n</i> -Hexane	510	150 (10%)	850 (60%)	3124 (30%)	1.5
PBPBD-DPG	<i>n</i> -Hexane	360	25 (91%)	102 (9%)		1.1
	<i>n</i> -Hexane	420	30 (77%)	105 (25%)		1.5
	<i>n</i> -Hexane	480	35 (67%)	100 (33%)		1.5
PBTBD-DMG	THF	500	45 (57%)	205 (29%)	920 (14%)	1.1
	THF	560	54 (75%)	220 (14%)	850 (18%)	1.2
PBTBD-DPG	THF	450	45 (72%)	200 (22%)	900 (6%)	1.4
	THF	490	38 (77%)	220 (15%)	805 (8%)	1.3
	THF	560	49 (76%)	204 (10%)	820 (14%)	1.3
PBPBD-DMG	THF	390	143 (52%)	811 (36%)	3600 (12%)	1.4
	THF	450	145 (31%)	850 (41%)	3219 (23%)	1.5
	THF	600	144 (17%)	820 (39%)	3550 (44%)	1.4
PBPBD-DPG	THF	360	20 (82%)	124 (18%)		1.3
	THF	420	25 (77%)	110 (23%)		1.3
	THF	480	27 (76%)	105 (24%)		1.2

$I(t) = A_1 \exp(-t/\tau_1) + A_2 \exp(-t/\tau_2) + A_3 \exp(-t/\tau_3)$ ;  $I(t)$ ,  $\lambda_{em}$ ,  $A$ , and  $\tau$  are the time-dependent fluorescence intensity, detection wavelength of emission, amplitude (noted as the normalized percentage in the parenthesis), and lifetime, respectively. The excitation wavelength of 298 nm was applied to all samples.

include phenylene do not show any significant dependence on the solvent polarity. The fluorescence lifetimes of the oligomers in each solvent are summarized in Table 1.

Generally, the conjugated polymers exhibit multiexponential decay characteristics as a result of various types of energy-transfer processes along the polymer chains as well as the distribution of the electronic levels and excited-energy trapping sites induced by inhomogeneities in the conformation.<sup>27</sup> The fluorescence decays of the polycarbogermanes also reveal multiexponential decay patterns, and the slow components become more significant at long wavelength regions in the emission spectra.<sup>28</sup>

As listed in Table 1, the decays in Figures 4 and 5 were fitted with multilifetime components. These lifetime values can provide the excited-state photophysics of the oligomers; however, they can also be misleading owing to their multilifetime components. Thus, we approximately discuss them in the following contents.

Table 1 indicates that PBTBD-DMG has fluorescence lifetimes of  $201 \pm 4$  ps ( $\tau_1$ ),  $631 \pm 10$  ps ( $\tau_2$ ), and  $1901 \pm 140$  ps ( $\tau_3$ ) in *n*-hexane as well as

$50 \pm 6$  ps ( $\tau_1$ ),  $213 \pm 11$  ps ( $\tau_2$ ),  $885 \pm 49$  ps ( $\tau_3$ ) in THF. PBTBD-DPG oligomer shows the fluorescence lifetimes of  $198 \pm 4$  ps ( $\tau_1$ ),  $613 \pm 11$  ps ( $\tau_2$ ),  $2775 \pm 106$  ps ( $\tau_3$ ) in *n*-hexane, and  $44 \pm 6$  ps ( $\tau_1$ ),  $208 \pm 11$  ps ( $\tau_2$ ), and  $842 \pm 51$  ps ( $\tau_3$ ) in THF. The fitted values for PBTBD oligomers indicate that the fluorescence lifetimes of the polycarbogermane oligomers do not significantly depend on the side-chain substituents of methyl or phenyl but sensitively depend on the solvent polarity of *n*-hexane or THF. The decay components in PBTBD-DMG and PBTBD-DPG oligomers of  $\sim 205$  ps ( $\tau_1$  in *n*-hexane and  $\tau_2$  in THF) do not depend on the solvent polarity, and they are comparable to the fluorescence lifetimes of poly(2,5-diethynylthiophene) (PDET) in a previous study in which the  $\pi$ - $\pi^*$  local excited-state lifetimes of PDET were two-exponential decay characteristics of  $139 \pm 5$  and  $205 \pm 3$  ps.<sup>29</sup> However, the other fluorescence lifetimes of these oligomers are significantly influenced by the solvent polarity.

The fluorescence lifetime of  $\sim 624$  ps ( $\tau_2$ ) in *n*-hexane seems to be changed to  $\sim 46$  ps ( $\tau_1$ ) in THF by considering their relative amplitudes at some detection wavelengths. The relatively fast

decay components (PBTBD-DMG:  $50 \pm 6$  ps, PBTBD-DPG:  $44 \pm 6$  ps) in THF solvent did not appear in previous research on PDET, which is the thiophene–diacetylene copolymer.<sup>29</sup> Therefore, these fast decay components in the PBTBD oligomers seem to have originated from the effect of the germanium atom introduction into the thiophene–diacetylene copolymer backbone in polar environment (THF). In these oligomers, the solvent polarity significantly influences the fluorescence lifetimes as well as the fluorescence spectra. It agrees well with typical characteristics of intramolecular charge-transfer (ICT) emission in previous reports.<sup>30,31</sup> Because the silicon subgroup elements (Si, Ge, and Sn) have the vacant d orbital in the valence shell, they may act as an electron acceptor to the  $\pi$  system. The traditional elucidation of the  $\pi$ -acceptor properties of the silicon subgroup elements is based on the idea of (d-p)  $\pi$  conjugation.<sup>20,25,32</sup> According to a recent report on polycarbosilane oligomers,<sup>16</sup>  $\pi$  conjugation can be extended, although the silicon atom by the ICT process was formed by (d-p)  $\pi$  conjugation<sup>17,18</sup> and the inductive effect in the  $\pi$ -conjugated oligomers including silicon atoms. Contrary to the polycarbogermane oligomers, polycarbosilane oligomers remarkably depend on the side-chain substituents of methyl or phenyl.<sup>16</sup> As a possible reason, it can be expected that the empty 4d orbital of the germanium atom does not efficiently overlap with the 2p orbital of the branched phenyl ring as compared with the empty 3d orbital of the silicon atom because the orbital of the germanium atom ( $[\text{Ar}]4s^24p^24d^0$ ) in the valence shell diffuses more than that of the silicon atom ( $[\text{Ne}]3s^23p^23d^0$ ) does.

Contrary to the thiophene-containing oligomers, the fluorescence lifetimes of PBPBD-DMG and PBPBD-DPG oligomers were not significantly influenced by solvent polarity. In PBPBD-DMG oligomer, the fluorescence lifetimes are  $143 \pm 10$  ps ( $\tau_1$ ),  $858 \pm 14$  ps ( $\tau_2$ ), and  $2900 \pm 197$  ps ( $\tau_3$ ) in *n*-hexane as well as  $144 \pm 1$  ps ( $\tau_1$ ),  $827 \pm 20$  ps ( $\tau_2$ ), and  $3456 \pm 207$  ps ( $\tau_3$ ) in THF. PBPBD-DPG oligomer shows the fluorescence lifetimes of  $30 \pm 5$  ps ( $\tau_1$ ) and  $102 \pm 3$  ps ( $\tau_2$ ) in *n*-hexane as well as  $24 \pm 4$  ps ( $\tau_1$ ) and  $113 \pm 10$  ps ( $\tau_2$ ) in THF. However, for PBPBD-DPG oligomer it is difficult to compare their fluorescence lifetimes with those of the others because the number of repeating units of PBPBD-DPG oligomer ( $n = 2$ ) is much shorter than those of the others ( $n = 33, 12,$  and  $36$ ). The thiophene group in PBTBD oligomers has a relatively richer elec-

tron density than the phenylene group. Moreover, the  $\pi$  clouds above and below the plane of the thiophene ring are possibly more diffused and polar than those of the phenyl ring because of the contribution of the sulfur atom ( $[\text{Ne}]3s^23p^4$ ) to the  $\pi$  clouds. On the basis of such discussion points, one can expect that the electron-donating ability of the  $\pi$ -conjugated backbone of PBTBD oligomers is relatively larger because of the thiophene groups than that of the  $\pi$ -conjugated backbone of PBPBD oligomers. In PBPBD oligomers, therefore, there is little possibility of the existence of the significant ICT state between the  $\pi$ -conjugated backbone and the germanium atom. On the other hand, in the case of PBTBD oligomers, the photoexcited electrons can be efficiently transferred from the  $\pi$ -electron system to the unoccupied 4d orbitals of the germanium atom by (d-p)  $\pi$  conjugation, which induces ICT states.

As shown in Table 1, the slowest decay components of the fluorescence lifetimes from a nanosecond to a few nanoseconds scale (0.8–3.6 ns) appear in the polycarbogermane oligomers with relatively long chain lengths, such as PBTBD-DMG ( $n = 33$ ), PBPBD-DMG ( $n = 36$ ), and PBPBD-DMG ( $n = 12$ ), but they do not appear in PBPBD-DPG oligomer ( $n = 2$ ). This suggests that these slowest decay components may be due to inter- or intramolecular aggregation effects among the  $\pi$ -conjugated backbones with long chains.

We can also confirm the ICT emission states in the polycarbogermane (PBTBD-DMG and PBTBD-DPG) oligomers containing thiophene with the fluorescence lifetimes and their amplitudes, which are listed in Table 1. Although the intensity of the steady-state fluorescence spectra at the respective lifetime component is proportional to  $a_i\tau_i$ , their positions in the steady-state spectra are approximately probed by monitoring the relative amplitudes of the lifetime components at the respective detection wavelengths.

For PBTBD oligomers in both solvents, in Table 1 the relative amplitude of the lifetime component of  $\sim 205$  ps decreases by changing the detection wavelength from the short- to the long-wavelength region. It indicates that the lifetime component of  $\sim 205$  ps corresponds to the emission in the short-wavelength region of the steady-state fluorescence spectra. This  $\sim 205$  ps lifetime component does not depend on the side-chain substitution effect as indicated in Table 1, whereas its relative amplitude decreases by changing the

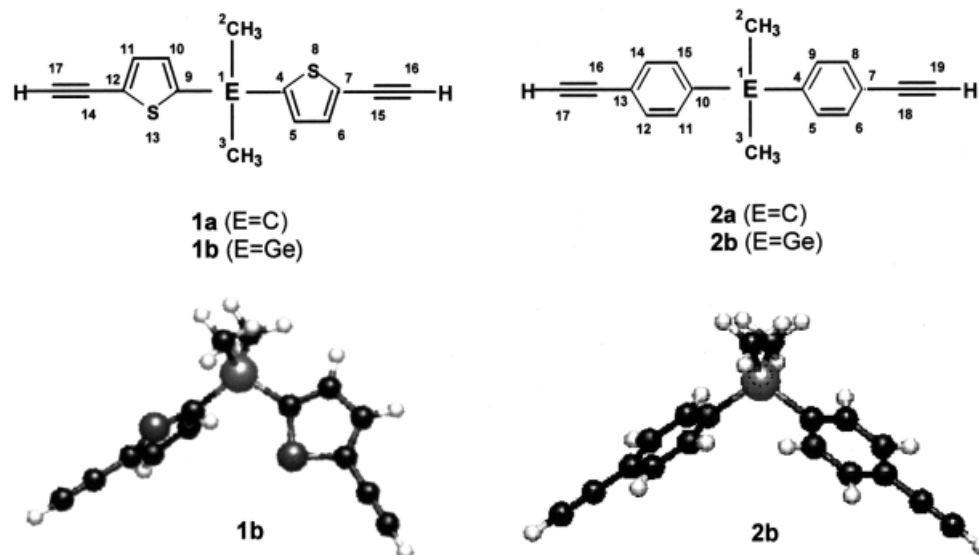


**Figure 6.** Chemical structures of the model compounds (**1a**, **1b**, **2a**, and **2b**) and energy-minimized conformations of the repeating units for PBTBD-DMG (**1b**) and PBPBD-DMG (**2b**).

solvent polarity from *n*-hexane to THF. Therefore, it is suggested that this component originates from the local  $\pi$ - $\pi^*$  excited-state emission of the diacetylene–thiophene copolymer backbone of the PBTBD oligomers, which is also comparable to the fluorescence lifetimes ( $139 \pm 5$  and  $205 \pm 3$  ps) reported in a previous study on PDET oligomers.<sup>29</sup> On the basis of the relative amplitude ratios of each lifetime component listed in Table 1, it is considered that the lifetime of  $\sim 620$  ps ( $\tau_2$ ) in *n*-hexane seems to be changed to  $\sim 46$  ps in THF. Contrary to the  $\sim 205$  ps lifetime component, such a lifetime change that depends on the solvent polarity occurs with an increase of the corresponding amplitude. It implies that the emission of this lifetime component is from the ICT emission states of the PBTBD oligomers and is responsible for the bathochromic shifts of the fluorescence spectra in Figures 3(b,c). The components with the slow lifetimes of  $\sim 0.8$  and  $\sim 3.6$  ns in Table 1 are probably due to the lower trap states induced by the long chains of the oligomers.

### Quantum Chemical Calculation

Quantum chemical calculations for the model compounds (Fig. 6 **1a**, **1b**, **2a**, and **2b**) were carried out in their ground as well as excited states on an IBM586-type computer using MOPAC97 to demonstrate the possibility of (d-p)  $\pi$  conjugation in the compounds of the silicon subgroup ele-

ments.<sup>33</sup> Although all calculations were performed in gas phase environments, they still provide valuable information supporting the experimental results. Figure 6 shows the chemical structures and the energy-minimized conformations of the repeating units of PBTBD-DMG (**1b**) and PBPBD-DMG (**2b**) in ground states obtained by the AM1 method.

The relative HOMO (highest occupied molecular orbital) and LUMO (lowest unoccupied molecular orbital) energy levels for **1a**, **1b**, **2a**, and **2b** obtained using the semiempirical CNDO/2 calculations are also illustrated in Figure 7. It suggests that the substitution of the germanium atom for the carbon atom induces the band gaps between HOMO and LUMO of **1b** and **2b** is decreased. Therefore, the introduction of the germanium atom into the backbone instead of the carbon atom produces new hybridized energy levels such as higher-lying HOMO and lower-lying LUMO through hybridization of the orbitals of the germanium atom and  $\pi$  orbitals of the adjacent  $\pi$  system. Such reductions of the band gap can be related to newly appeared absorption bands in the long-wavelength region as shown in Figure 3. The reduction of the band gap ( $\Delta$ band gap = 3.1 eV) in the thiophene-containing compounds (**1a** and **1b**) is larger than that ( $\Delta$ band gap = 2.4 eV) in the phenylene-containing compounds (**2a** and **2b**). It implies that the introduction effect of the germanium atom is larger in the thiophene-con-

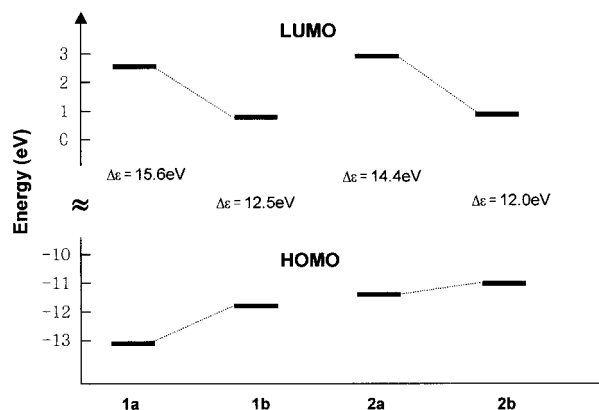


**Figure 7.** Relative HOMO and LUMO energy levels for **1a**, **1b**, **2a**, and **2b** obtained by the semiempirical CNDO/2 calculations.  $\Delta\epsilon$  is the band gap between the HOMO and LUMO energy levels.

taining  $\pi$ -conjugated backbone than the phenylene-containing  $\pi$ -conjugated backbone, which is consistent with the experimental results.

As shown in Figure 6, the conformations of two models with the germanium atom are close to a tetrahedral geometry. The appropriate orientation of d orbitals of the central atom for the maximum interaction with several  $\pi$  systems depends strongly on the number of adjacent  $\pi$  systems.<sup>34,35</sup> For these molecules, the d orbitals of the germanium atom are appropriately arranged in their orientation to have maximum interaction with the  $\pi$  orbitals of two aromatic groups. If the  $p_\pi$  orbitals of the aromatic groups lie in the  $xy$  plane (i.e., the plane of the aromatic groups is perpendicular to the  $xy$  plane), the effective orbital overlap between  $p_\pi$  orbitals of aromatic groups in the  $xy$  plane and  $d_{xy}$  of the germanium atom can exist as shown in Figure 8. Therefore, although there are two aromatic planes that are nearly orthogonal in their structure, the  $p_\pi$  orbital of each aromatic group can still maintain the effective overlap with  $d_{xz}$  or  $d_{yz}$  orbitals of the germanium atom in the  $xz$  plane or the  $yz$  plane, respectively. According to the results from the semiempirical calculations, the dihedral angles of C4-Ge1-C9-C10 (C4-Ge1-C9-S13) and C9-Ge1-C4-C5 (C9-Ge1-C4-S8) in **1b** are  $80.5^\circ$  ( $-99.5^\circ$ ) and  $-157.6^\circ$  ( $22.7^\circ$ ), respectively, and the angles of C4-Ge1-C10-C15 (C4-Ge1-C10-C11) and C10-Ge1-C4-C5 (C10-Ge1-C4-C9) in **2b** are  $65.8^\circ$  ( $-114.1^\circ$ ) and  $-67.3^\circ$  ( $112.5^\circ$ ), respectively. In the case of **1b**, one of two thiophene groups is almost perpendicular to the  $xy$  plane, and the other is approximately planar to the  $xy$  plane. As men-

tioned previously, for both of the perpendicular and planar forms, the effective orbital overlaps between  $p_\pi$  orbitals of the thiophene groups and d orbitals of the germanium atom are possible. However, in the conformations of **2b**,  $p_\pi$  orbitals of phenylene groups cannot sufficiently overlap with the d orbitals of the germanium atom as much as the case of **1b**. Such theoretical results support the previous experimental discussion that more effective (d-p)  $\pi$  conjugation through the overlap of the p orbitals in the  $\pi$  system and the vacant 4d orbitals in the germanium atom exists in the thiophene-containing oligomers (PBTBD-DMG and PBTBD-DPG) as compared with the phenylene-containing oligomers (PB-PBD-DMG and PBPBD-DPG). Although the conformation in Figure 6 was calculated in the ground state, it can be expected that there is a greater chance for the thiophene-containing oligomers, in their photoexcited states, to have the (d-p)  $\pi$  conjugation through the sufficient overlap between the p orbital of the  $\pi$  system and the 4d orbital of the germanium atom because the conformation in the ground state seems to be similar to that in the initially excited Franck–Condon state.

## CONCLUSION

In the case of PBTBD oligomers, the solvent polarity becomes an important factor to the emis-

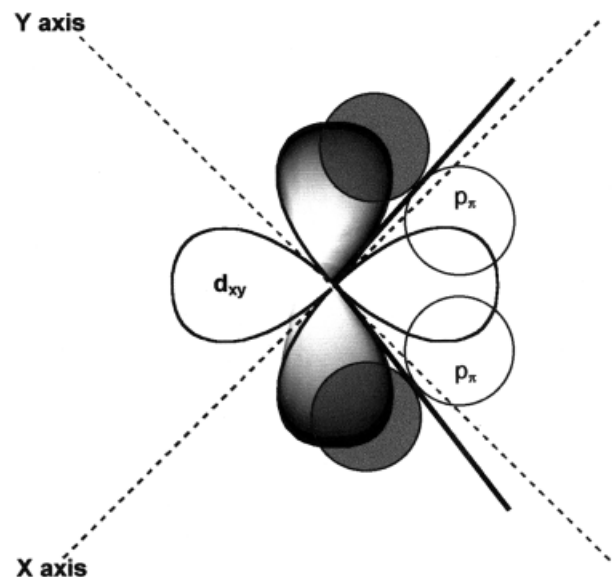


**Figure 8.** Effective orbital overlap between  $d_{xy}$  and  $p_\pi$  orbitals in the  $xy$  plane. The solid line represents the sigma bond between the germanium atom and the carbon atom in the aromatic group.



sion lifetimes and fluorescence energy states, whereas for PBPBD oligomers, the results from the steady-state and time-resolved fluorescence measurements do not show the solvent polarity-dependent characteristics. There are significant redshifts in the steady-state fluorescence spectra of PBTBD-DMG and PBTBD-DPG oligomers with increasing solvent polarity. The picosecond fluorescence-decay profiles of these compounds in polar solvent (THF) reveals the fast decay components of  $\sim 46$  ps ( $\tau_1$ ), which has not been observed in the PDET copolymer. This component seems to become  $\sim 624$  ps ( $\tau_2$ ) in *n*-hexane solvent. It suggests that the solvent-polarity dependence of the lifetimes is due to the ICT states that are induced by the germanium atom and the thiophene-containing  $\pi$ -conjugated backbone. It also agrees well with typical characteristics of ICT emissions in previous reports.<sup>30,31</sup> The results of quantum chemical calculations by AM1 and CNDO/2 methods imply that the vacant 4d orbitals of the germanium atom overlap more efficiently with the p orbitals of the thiophene-containing  $\pi$ -conjugated backbone that are more diffused, electron rich, and polar than those of the phenylene-containing  $\pi$ -conjugated backbone. Therefore, the ICT emission states in PBTBD-DMG and PBTBD-DPG oligomers are induced possibly by the excited-state electron-transfer process from the thiophene-containing  $\pi$ -conjugated backbone to the unoccupied 4d orbital of the germanium atom through (d-p)  $\pi$  conjugation.

This research was financially supported by KRF (BSRI DP0228) and CRM-KOSEF (1998G0102), South Korea. Y. T. Park thanks the Korea Science and Engineering Foundation (KOSEF 95-0501-02-01-3) for their financial support.

## REFERENCES AND NOTES

- Lauchlan, L.; Etemad, S.; Chung, T. C.; Heeger, A. J.; MacDiarmid, A. G. *Phys Rev B* 1981, 24, 3701.
- Kobayashi, T.; Yoshizawa, M.; Stamm, U.; Taiji, M.; Hasegawa, M. *J Opt Soc Am B* 1990, 7, 1558.
- Fichou, D.; Horowitz, G.; Xu, B.; Garnier, F. *Synth Met* 1990, 39, 243.
- Tour, J. M. *Chem Rev* 1996, 96, 537.
- Stevens, M. P. *Polymer Chemistry*; Oxford University Press: New York, 1999.
- Kaufman, J. H.; Chung, T. C.; Heeger, A. J.; Wudi, F. J. *J Electrochem Soc* 1984, 131, 2092.
- Dodabalapur, A.; Toris, L.; Katz, H. E. *Science* 1995, 268, 270.
- Gill, R. E.; Malliaras, G. G.; Wildeman, J.; Hadziioannou, G. *Adv Mater* 1994, 6, 132.
- Noma, N.; Tsuzuki, T.; Shirota, Y. *Adv Mater* 1995, 7, 647.
- Timothy, M. S.; Chroline, J. G.; Mark, S. W. *J Phys Chem* 1995, 99, 4886.
- Zeigler, J. M.; Harrah, L. A.; Johnson, A. W. *Proc SPIE Int Soc Opt Eng* 1985, 539, 166.
- Kunai, A.; Ueda, T.; Horata, K.; Toyoda, E.; Nagamoto, I.; Ohshita, J.; Ishikawa, M.; Tanaka, K. *Organometallics* 1996, 15, 2000.
- Malliaras, G. G.; Herrema, J. K.; Wildeman, J.; Wieringa, R. H.; Gill, R. E.; Lampoura, S. S.; Hadziioannou, G. *Adv Mater* 1993, 5, 721.
- Bréfort, J. L.; Corriu, R. J. P.; Gerbier, Ph.; Guérin, C.; Henner, B. J. L.; Jean, A.; Kuhlmann, Th. *Organometallics* 1992, 11, 2500.
- Bae, J. Y.; Kim, Y.-R.; Park, Y. T. *Bull Korean Chem Soc* 2000, 21, 831.
- Hwang, I.-W.; Song, N. W.; Park, Y. T.; Kim, Y.-R. *J Polym Sci Part B: Polym Phys* 1999, 37, 2901.
- Shizuka, H.; Ueki, Y.; Ishikawa, M.; Kumada, M. *J Chem Soc Faraday Trans 1* 1984, 80, 341.
- Yamamoto, M.; Kudo, T.; Ishikawa, M.; Tobita, S.; Shizuka, H. *J Phys Chem A* 1999, 103, 3144.
- Sakurai, H.; Sugiyama, H.; Kira, M. *J Phys Chem* 1990, 94, 1837.
- Egorochkin, A. N. *Russ Chem Rev* 1984, 53, 445.
- Dewar, M. J. S.; Zoebisch, E. G.; Healy, E.; Stewart, J. J. P. *J Am Chem Soc* 1985, 107, 3902.
- Popel, J. A.; Segal, G. A. *J Chem Phys* 1966, 44, 3289.
- Hwang, I.-W.; Choi, H. H.; Cho, B. K.; Lee, M.; Kim, Y.-R. *Chem Phys Lett* 2000, 325, 219.
- Dewar, M. J. S.; Thiel, W. *J Am Chem Soc* 1977, 99, 4499.
- Egorochkin, A. N.; Khorshev, S. Ya. *Russ Chem Rev* 1980, 49, 820.
- Nishinaga, T.; Komatsu, K.; Sugita, N. *J Org Chem* 1995, 60, 1309.
- Wilson, W. L.; Weidman, T. W. *J Phys Chem* 1991, 95, 4568.
- Guillet, J. E.; Hoyle, C. E.; MacCallum, J. R. *Chem Phys Lett* 1978, 54, 337.
- Hwang, I.-W.; Song, N. W.; Park, Y. T.; Kim, Y.-R. *Eur Polym J* 1998, 34, 335.
- Bhattacharyya, K.; Chowdhury, M. *Chem Rev* 1993, 93, 507.
- Rettig, W. *Angew Chem Int Ed Engl* 1986, 25, 971.
- Pauling, L. *The Nature of the Chemical Bond*; Cornell University Press: Ithaca, New York, 1948.
- Craig, D. P.; Maccoll, A.; Nyholm, R. S.; Orgel, L. E.; Sutlon, L. E. *J Chem Soc* 1954, 332.
- Jaffé, H. H. *J Phys Chem* 1954, 58, 185.
- Ebsworth, E. A. V. In *Organometallic Compounds of the Group IV Elements the Bond to Carbon*; MacDiarmid, A. G., Ed.; Marcel Dekker: New York, 1968; Vol. 1, p 1.